



7

UNIVERSITY OF ICELAND

Dynamical Corrections to the Transition State Theory for Magnetic Systems

Author:

Olga Ástríður Guðnadóttir

Advisors:

Pavel Bessarab

Hannes Jónsson

February 16, 2018

Contents

1	Introduction	3
2	Two-step method for calculating the rate constant	4
	Transition state theory for multiple spins	4
	Correction to HTST by direct simulation	7
3	Application	7
	Model	7
	Spin dynamics	8
	Kramers/Langer	8
	Kalmykov	9
	HTST	9
	Correction calculations	9
4	Conclusions	10

1 Introduction

The study of the stability of magnetic systems, such as hard drives and magnetic recording devices, is of importance both as it pertains to a fundamental description of micromagnetism and to the design of technology relying on magnetism. The magnetic state of a solid can be described by the orientation of magnetic dipole moments within it.

Stable states correspond to certain orientations of these that minimize the potential energy, which stems from anisotropy, magnetic fields and interaction with other magnetic moments. The anisotropy can depend both on the shape of the sample of the solid (shape anisotropy) and on the shape of the crystal lattice of the solid (magnetocrystalline anisotropy) and the fields can be either external or due to the sample itself. The magnetic state of a sample can be altered by applying external magnetic fields that will change the potential energy temporarily and thus induce a rotation of magnetic moments, that then relax back into the same or a different potential energy minimum once the external field is removed. The potential energy of a magnetic moment during a transition between two stable states is illustrated in figure 1, which shows a macrospin with anisotropy easy axis (lowest energy state) along the z-axis. As the macrospin rotates from the energy minimum corresponding to the state in which it is aligned with the z-axis and pointing upward, through the state where it is orthogonal to the z-axis, to the other energy minimum, corresponding to the state where the macrospin is aligned with the z-axis but pointing downward, the potential energy first increases and then decreases. At finite temperatures, transitions between stable states can also be induced by thermal fluctuations in the system, that give the spin enough energy to overcome the potential barrier between them.

The thermal stability of a system is characterized by the average lifetime, i.e. the average time it spends in a particular stable state before it transitions into another. Its inverse, the rate at which thermally induced transitions take place follows the empirical rate law associated with Arrhenius

$$k = k_0 e^{-\frac{\Delta E}{k_B T}} \quad (1)$$

where k is the rate constant (transitions per unit time), k_0 is the so-called pre-factor or attempt frequency, ΔE is the potential energy barrier between minima and k_B is the Boltzmann constant.

In theory, it is straightforward to determine the rate constant of any transition by direct simulation of the time evolution of the system. For magnetic system at finite temperatures, this can be done by integration of the stochastic Landau-Lifshitz-Gilbert equation,

$$\frac{d\mathbf{m}_i}{dt} = -\gamma \mathbf{m}_i \times [\mathbf{B}_i + \mathbf{b}_i(t)] - \gamma \frac{\alpha}{m} \mathbf{m}_i \times (\mathbf{m}_i \times [\mathbf{B}_i + \mathbf{b}_i(t)]) \quad (2)$$

where \mathbf{m}_i is the i -th magnetic moment, $\mathbf{B}_i + \mathbf{b}_i(t)$ is the effective field felt by the i -th magnetic moment and α is a dimensionless damping parameter. The time dependent term in the effective field is a stochastic term simulating the thermal fluctuations of the system. In practice, however, this approach is unfeasible or even altogether impossible for systems in which the transitions are rare compared to the fluctuations in the system. When the transitions are rare, the simulation time has to be increased to allow for enough

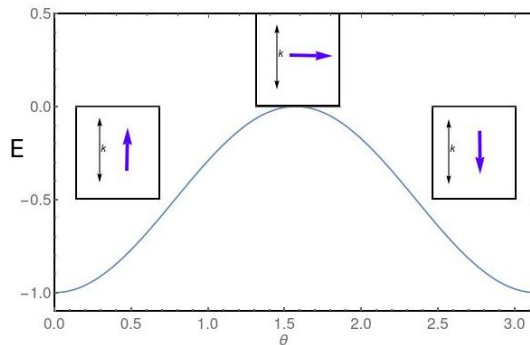


Figure 1: The uniaxial anisotropy energy of a magnetic moment as it transitions from one energy minimum to another. The inserts show the orientation of the spin and the anisotropy easy axis at different points in the transition.

transitions to obtain a statistically significant value of the transition rate. However, the time step cannot be increased since it needs to be small enough to resolve the fluctuations of the system. Because of this separation of time scales, the computing power needed for a direct simulation of rare events grows with average lifetime and can become impossibly long.

The separation of time scales also opens up the possibility of using statistical methods, however, such as Transition State Theory (TST) and Kramers/Langer's method. Within these theories, the rate is found by evaluation of the average flux through a dividing surface that separates the initial state and the final state in configuration space. This can be visualized on a potential energy surface such as that in figure 2. To each transition corresponds a trajectory starting in the vicinity of one minimum (the initial state) and going to the vicinity of another (the final state), where it stays for a long time compared to the relaxation time of the system. Clearly, all trajectories corresponding to a transition cross the dividing surface at least once. Transition state theory takes the rate constant to be the rate at which the trajectories cross the dividing surface, and thus gives an upper bound for the rate of transitions (see figure 2).

Kramers' theory, generalized to multiple degrees of freedom by Langer, corrects for the recrossing of the dividing surface by incorporating Brownian motion in a parabolic potential into the expression for the rate constant. While this gives a better approximation than TST when the potential barrier is indeed parabolic, it cannot be used at all if a harmonic approximation of the energy barrier is not valid. As an example, this is the case for flat energy barriers, for which the Kramers/Langer rate constant vanishes. Nevertheless, flat barriers become important in e.g. the description of domain walls. TST, on the other hand, makes no attempt at correcting for the recrossings, meaning that the correction can be done separately, in a second step. It is known that the exact rate can be written as a product of this estimate k^{TST} and a correction factor [7] [3]

$$k = \kappa k^{TST} \quad (3)$$

where κ is a factor between 0 and 1 that corrects for the recrossings of the dividing surface. It can be exactly evaluated by simulating the dynamics of the system around the dividing surface as demonstrated by Keck for two-state atomistic systems [5] and many-state atomistic systems by Voter and Doll [7].

The statistical methods have been derived for a wide variety of systems. Particularly, the theoretical treatment of spin systems began with Néel, who calculated the reversal rate of the magnetization of a small magnetic particle within the TST framework. He described the magnetic moment of the particle as a macrospin with uniaxial anisotropy (one easy axis). When there is no external field, the potential energy is the anisotropy energy, which is axially symmetric. The transition can therefore be described by only one coordinate (figure 1).

Brown further developed this theory by using Kramers' method to obtain a rate constant for the same transition. Klik and Gunther then extended the treatment to an arbitrary shape of the potential that the macrospin was subject to by using Langer's generalization of Kramers' theory. When the potential is due to anisotropy and an external homogeneous magnetic field, an exact analytical expression for the rate has been obtained [4]. A harmonic approximation to TST has also been formulated for systems with multiple spins [2]. The aim of this work is to describe the calculation of the dynamical correction factor introduced above for this case. I present results of the implementation of the algorithm, as well as the results obtained for the same system with other statistical methods and direct simulations.

2 Two-step method for calculating the rate constant

Transition state theory for multiple spins As mentioned above, a derivation of TST (in the harmonic approximation) for systems consisting of multiple spins is given in [2] and will be repeated here. The coordinates describing the system are taken to be the polar angle θ_i and azimuthal angle ϕ_i of each spin, so the system as a whole is described by the vector $\mathbf{x} = \{\boldsymbol{\theta}, \boldsymbol{\phi}\}$. The TST rate constant in this case is given by

$$k^{TST} = \frac{1}{C} \int_A e^{-E(\mathbf{x})/k_B T} \delta[f(\mathbf{x})] v_{\perp}(\mathbf{x}) h(v_{\perp}(\mathbf{x})) J(\mathbf{x}) d\mathbf{x} \quad (4)$$

where A denotes the region associated with the initial state up to and including the dividing surface, E is the total energy of the system, $f(\mathbf{x})$ is a function defining the dividing surface by $f(\mathbf{x}) = 0$, $J(\mathbf{x}) = \prod_i M_i^2(\theta, \phi) \sin \theta_i$ is the Jacobian determinant for the change of coordinates from cartesian to spherical and v_{\perp} is the velocity perpendicular to the transition state, which depends only on the coordinates $\mathbf{x} = \{\boldsymbol{\theta}, \boldsymbol{\phi}\}$ in magnetic systems. The delta function ensures that the integral is taken only over the

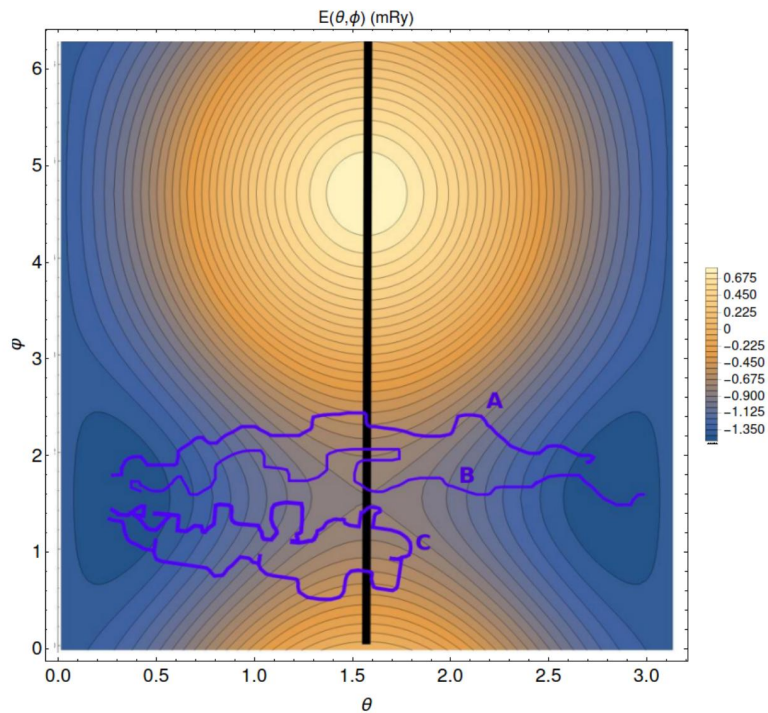


Figure 2: Contour plot of an energy surface. Two equivalent minima can be seen, as well as a saddle point. The black line shows the placement of the dividing surface utilized in TST. Three different types of trajectories (A,B,C) are shown in blue. Trajectory A goes straight from the initial state (taken to be to the left) to the final state through the dividing surface, while B and C recross the dividing surface once they have left it. In the case of B, the trajectory is counted as two transitions when in reality there is only one, and in the case of C the trajectory is counted as a transition although nonw has taken place.

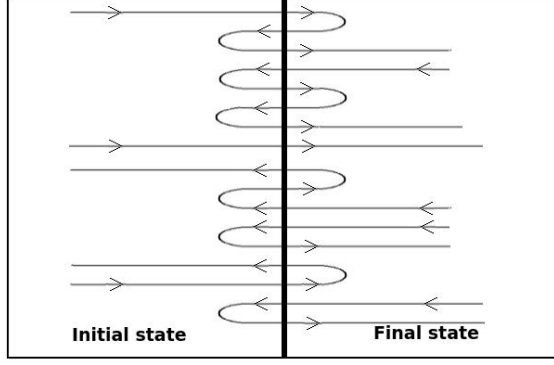


Figure 3: Schematic representation of the algorithm described in [7]. The black line in the middle indicates the dividing surface, and the flux through it is shown schematically. By assigning -1 to all lines leaving the dividing surface to the left and +1 to the ones going to the right, it is clear that the sum of those that end up in the final state is equal to the actual number of transitions. It can be understood by examining the trajectories; for each trajectory with value +1 corresponding to a recrossing, there is a trajectory with value -1 that negates it.

transition state and the Heaviside step function, h , ensures that it counts only the flux out of the initial state and not into it. $\frac{1}{C}$ is a normalization factor given by

$$C = \int_A e^{-E(\mathbf{x})/k_B T} J(\mathbf{x}) d\mathbf{x} \quad (5)$$

In the adiabatic limit, the Landau-Lifshitz-Gilbert equations 2 can be separated. If we further assume low damping, they can be written as

$$(1 + \alpha^2) \sin \theta_i \dot{\phi}_i = \frac{\gamma}{M_i} \left(\frac{\partial E}{\partial \theta_i} - \frac{\alpha}{\sin \theta_i} \frac{\partial E}{\partial \phi_i} \right) \quad (6)$$

$$(1 + \alpha^2) \sin \theta_i \dot{\theta}_i = -\frac{\gamma}{M_i} \left(\frac{\partial E}{\partial \phi_i} + \alpha \sin \theta_i \frac{\partial E}{\partial \theta_i} \right) \quad (7)$$

When the potential energy function is sufficiently smooth around the minimum and saddle point it can be expressed by a second order expansion in the normal mode coordinates (displacements along the eigenvectors of the Hessian of the energy function). This can be written as

$$E_\beta(\mathbf{q}) = E_\beta(0) + \frac{1}{2} \sum_{j=1}^D a_{\beta,j} q_{\beta,j}^2 \quad (8)$$

at the minimum ($\beta = m$) and the saddlepoint ($\beta = sp$). Now the velocity orthogonal to the dividing surface can be written as

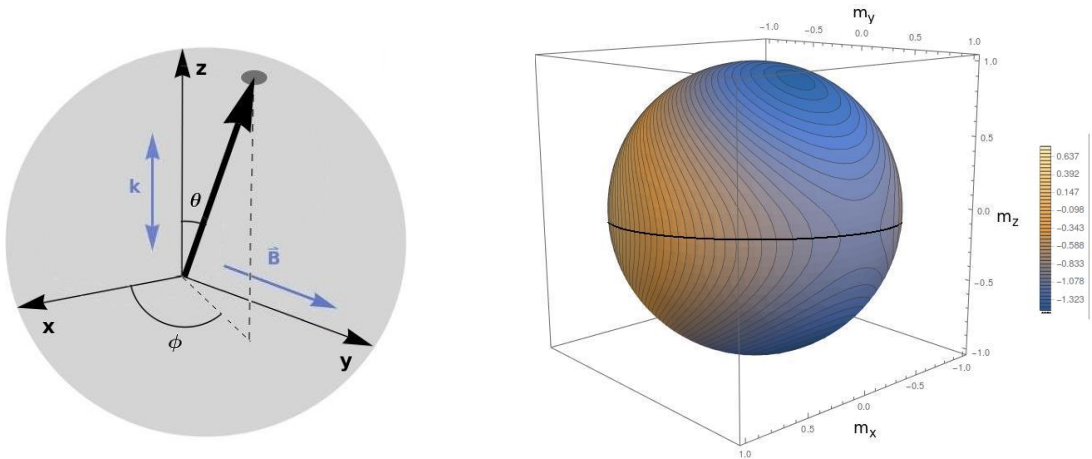
$$v_\perp = \dot{q}_{sp,1} = \sum_{j=2}^D a_j q_{sp,j} \quad (9)$$

where $q_{sp,1}$ is the coordinate corresponding to the eigenvector of the Hessian which is orthogonal to the dividing surface. All eigenvectors of the Hessian are chosen so that $a_i > 0$ leads to a positive contribution to v_\perp .

When the rate constant is evaluated with this approximation (see [1] for details) the rate constant becomes

$$k^{HTST} = \frac{1}{(1 + \alpha^2)} \frac{1}{2\pi} \frac{J_s}{J_m} \sqrt{\frac{\sum_{j=2}^D a_j^2 \prod_{i=1}^D \sqrt{\epsilon_{m,i}}}{\epsilon_{sp,j} \prod_{i=2}^D \sqrt{\epsilon_{sp,i}}}} \quad (10)$$

where $\epsilon_{m,i}$ and $\epsilon_{s,i}$ are the eigenvalues of the Hessian at the minimum and saddle point, respectively and a_j is the j -th expansion coefficient of the velocity in terms of the normal mode coordinates.



(a) The system under study consists of a macrospin with easy axis in the z -direction subject to an external field in the y -direction. The figure also shows the polar angle θ and the azimuthal angle ϕ , which are the coordinates of the system.

(b) The tip of the macrospin will trace a sphere, each point on the sphere corresponding to a unique pair of the variables θ and ϕ . Here the potential energy as a function of θ and ϕ is superimposed on the sphere.

Figure 4: Model

Correction to HTST by direct simulation As mentioned in the introduction, TST overestimates the rate constant by counting every crossing of the dividing surface as a transition. The goal of the recrossing calculations is to determine how much of the flux through the surface corresponds to actual transitions. Figure 3 shows schematically what happens at the dividing surface, with trajectories coming from both the initial state and the final state. The points at which the trajectories cross the dividing surface will follow the Boltzmann distribution. The algorithm used for calculating the correction factor is described in [7]. Instead of using the long trajectories starting at the minima, we choose N points on the dividing surface as starting points for new trajectories to be simulated with spin dynamics. They are assigned the phase $\Theta = -1$ if they are headed to the initial state and $\Theta = +1$ if they are headed toward the final state. They are then followed until they settle in one of the minima and assigned a value $I = 1$ if they end up in the final state or $I = 0$ if they end up in the initial state. The corrected rate constant is given by

$$k = \kappa k^{HTST} \quad (11)$$

where

$$\kappa = \frac{2}{N} \sum_{j=1}^N \Theta(j) I(j) \quad (12)$$

which ensures that only trajectories that end in the final state are counted, and each recrossing negates a crossing, thus counting only one for each transition. The two critical parts of the implementation of the algorithm are assigning the phase at the start of the simulation and determining when a transition has taken place and the simulation should be terminated.

3 Application

In this section, the two step method is applied to a simple and instructive model identical to the one found in reference [6], in which Forward Flux Sampling is used to calculate the rate constant. The results are then compared to Forward Flux Sampling and various methods described in the introduction.

Model The model system is a uniaxial ferromagnetic particle, with anisotropy axis in the z -direction, subject to an external field in the positive y -direction. This system can be described by a macrospin as illustrated in figure 4a. Figure 4b shows (part of) the energy surface of this system as a function of the

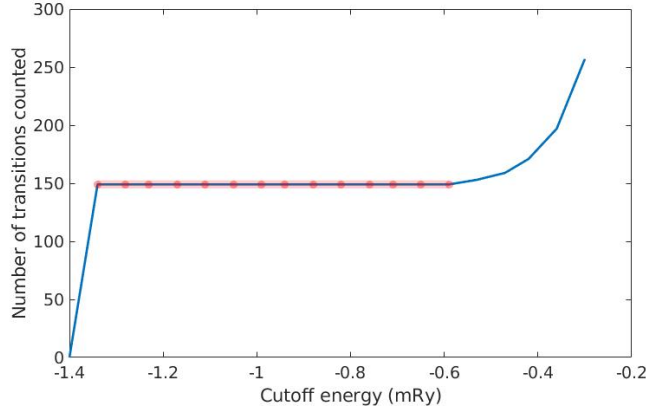


Figure 5: The number of transitions as counted with different values of the cutoff energy, ranging from the energy minimum to the saddle point. The red part of the graph shows the region where the rate constant is independent of the choice of cutoff energy.

orientation of the macrospin. This is the same energy surface that is shown in 2 as a function of the state variables θ and ϕ . The energy minima of this system correspond to the magnetic moment being parallel or antiparallel to the easy axis when the external field is zero, and move toward the y-axis when it is increase. The potential energy of the system is the sum of the anisotropy energy and the Zeeman energy

$$E = -k(\mathbf{e}_z \cdot \mathbf{m})^2 - \mathbf{M} \cdot \mathbf{B} \quad (13)$$

where k is the (positive) anisotropy constant, \mathbf{e}_z is the unit vector in the z-direction (the easy axis), \mathbf{m} is the unit vector in the direction of the magnetic moment, $\mathbf{M} = M\mathbf{m}$ is the magnetic moment and $\mathbf{B} = B\mathbf{e}_y$ is the external field. In spherical coordinates, this can be written as

$$E = -k \cos^2(\theta) - MB \sin(\theta) \sin(\phi) \quad (14)$$

For all cases, the anisotropy constant is $k = -1.38$ mRy, the magnitude of the macrospin is $42.9 \mu_B$ and the temperature is chosen so that $T = \frac{\Delta E}{9k_B}$. The damping and magnitude of the external field is varied.

Spin dynamics To obtain the rate constant from direct dynamics, the Landau-Lifshitz-Gilbert equations (2) are used to evolve the system in time and the transitions are counted. For a transition to have taken place, two conditions need to be satisfied:

1. the system is on the other side of the dividing surface compared to the state it last transitioned into and
2. the system is close the minimum on that side of the dividing surface.

To determine whether the system is close enough to the minimum, we used a cutoff energy value and counted a transition when the total energy of the system decreased below this value. Clearly, the transition rate can not depend on this choice of cutoff energy, so it has to be chosen in a region where the rate constant is independent of it. Figure 5 shows the rate constant as a function of the cutoff energy for a representative case.

Kramers/Langer For this particular system, rate constant within the Kramers/Langer framework is given by

$$k^{Langer} = \frac{1}{2\pi} \sqrt{\frac{-M^2 B^2 + 4k}{MB(2k - MB)}} \frac{\alpha\gamma}{M(1 + \alpha^2)} \left(1 + \sqrt{(-k + MB)^2 - 2(1 + \alpha^2)(-k + MB)} \right) e^{\frac{-E_{bar}}{k_B T}} \quad (15)$$

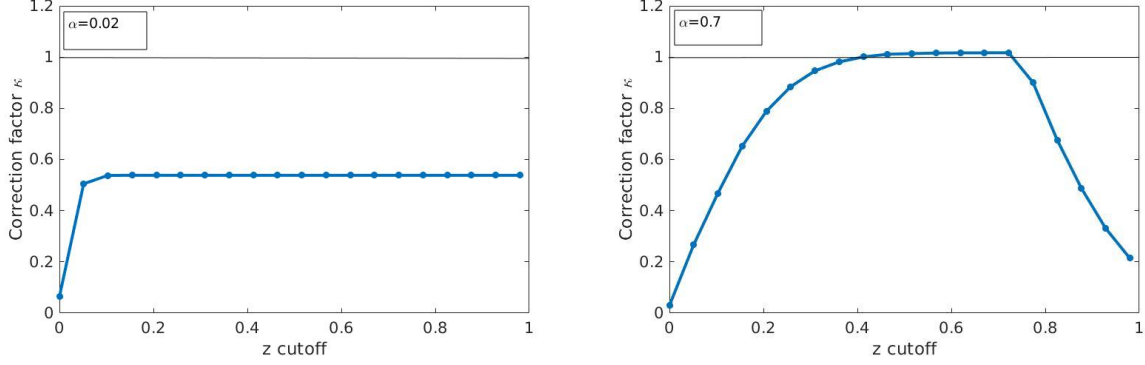


Figure 6

Kalmykov An exact analytical formula by Kalmykov was specifically derived for the case of a uniaxial ferromagnetic particle in an external magnetic field [4]. In the case when the external field is perpendicular to the easy axis, it simplifies to

$$k^{Kalmykov} = \frac{\sigma\sqrt{1+h}(1-2h+\sqrt{1+4h(1-h)\alpha^{-2}})A^2(\alpha(S_i))}{4\tau_N\pi\sqrt{h}e^{\sigma(1-h)^2}A(2\alpha S_i)}$$

where $\sigma = \beta k = \frac{Vk}{k_B T}$,

$h = \frac{BM}{2k}$, $A(\alpha S_i) = \exp\left(\frac{1}{\pi} \int_0^\infty \frac{\ln(1-\exp(-\alpha S_i(x^2+\frac{1}{4})))}{x^2+\frac{1}{4}} dx\right)$,

$S_i = 16\sigma\sqrt{h}\left[1 - \frac{13}{16}h + \frac{11}{8}h^2 - \frac{3}{16}h^3 + \frac{7}{384}h^4 + \frac{1}{256}h^5 + O(h^6)\right]$

and $\tau_N = \frac{\beta M(1+\alpha^2)}{2\gamma\alpha}$.

HTST At the saddlepoint, the Hessian of the energy (equation 14) in the basis $\{\theta, \phi\}$ is diagonal, so the normal mode coordinates coincide with θ and ϕ , with θ being orthogonal to the dividing surface. The velocity orthogonal to the dividing surface can thus be read directly from equation 7, and a can be determined by combining 7 and 9. Equation 10 becomes

$$k^{HTST} = \frac{-\gamma 2k^2}{(1+\alpha^2)M^2 B\pi} \sqrt{1 + \frac{M^2 B^2}{4k^2}} \exp\left(\frac{+4k^2 + 4kMB - M^2 B^2}{4kk_B T}\right) \quad (16)$$

Correction calculations The starting points of the trajectories were chosen by letting an ensemble of 29000 identical system reach equilibrium with a Metropolis algorithm. The trajectories were then simulated until they had reached one of the energy minima (a transition had taken place). A timestep of 10^{-14} or smaller was determined to be necessary for the error in the solution to be negligible as compared to the thermal fluctuations. To determine when a transition had taken place, the same method as in the full simulations (spin dynamics) was used. The value of the cutoff energy used was the same as previously determined by full simulations.

For assigning the phase, two methods were tested.

Method 1: In the first method, the phase was determined by the position of the starting point in the dividing surface. Since, in magnetic systems, the velocity is a function of position, this determined which way the velocity pointed. This was applied first to the the same cases as those studied in [6], with the damping parameter kept fixed at $\alpha = 0.02$ and the external field chosen so that it was 10%, 20%, 30% or 40% of the anisotropy field. The results of this can be seen in figure 8. Evidently, they agree well with the rate constant obtained in direct dynamics.

Next, the external field was kept fixed at 40% of the anisotropy field, and the damping parameter was varied from 0 to 0.7. The results are shown in figure 7. Here, again, we can see good correspondence between our results and the results from direct dynamics for small damping. As the damping increases above 0.4, we see a deviation from both the direct dynamics and Kalmykov's exact formula plotted on the same graph.

Method 2: In an attempt to circumvent the possible effect that the thermal fluctuations might have on the direction in which the spin leaves the dividing surface, as opposed to it being determined

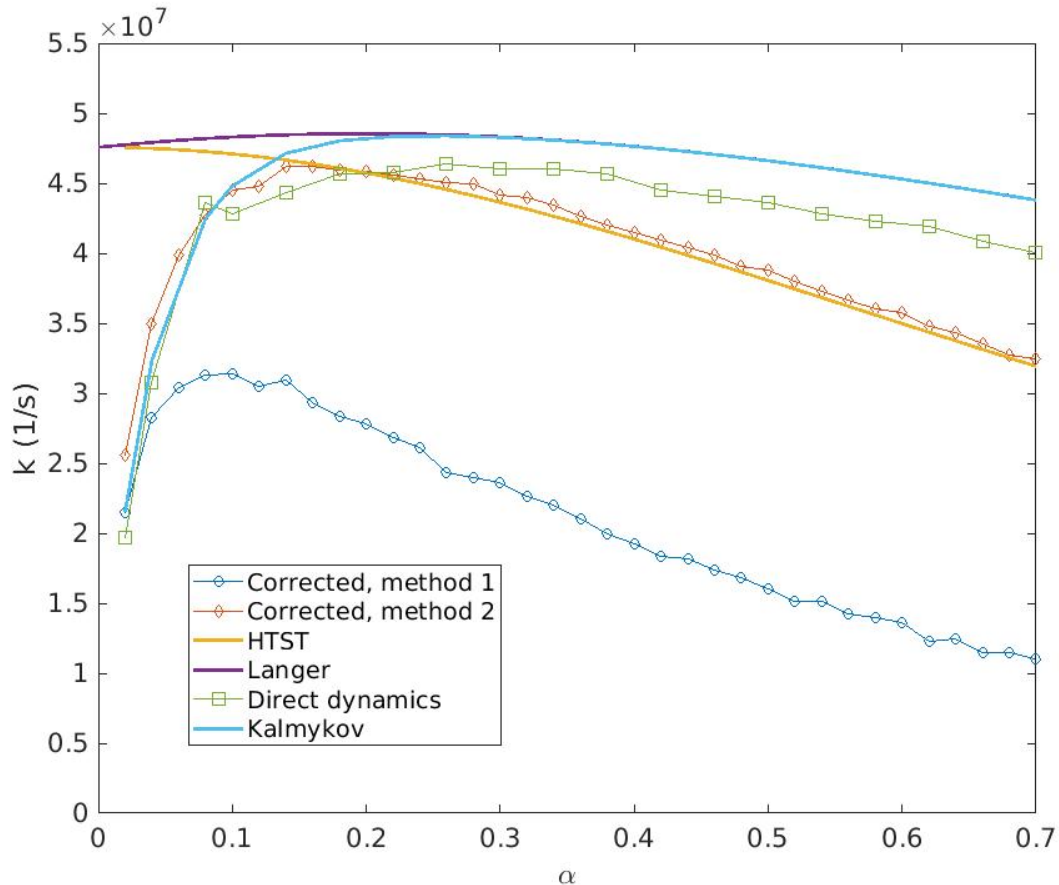


Figure 7: Results for the rate constant when the external field is fixed to $B = 0.4H_a$ and the damping parameter is varied. The results are obtained by the different methods described above.

completely by the position of the spin *in the dividing surface*, we simply assigned the phase according to the position of the spin *as soon as it left it*. This method is obviously very sensitive to noise right around the dividing surface, so we used a cutoff value of z , and assigned the phase as soon as the trajectory got a z value above or below this. By the same logic as when the energy cutoff value was chosen, we chose the z -value in an interval where the correction factor was independent of it (figure 6). The method was applied to the same cases as method 1, and shows a slightly worse agreement with other methods at low damping than method 1 did, but much better at higher damping. It is important to note, though, that method 2 gives a correction factor bigger than 1 for higher damping. This contradicts the fact that TST always gives an upper bound on the rate constant.

4 Conclusions

Though not all kinks have been worked out yet, the methods described above have the potential to be a most valuable tool once they have been. One thing to investigate is whether the HTST formulation derived in Methods is valid for higher damping. Another thing is to find out how come the correction factor becomes larger than 1 for some cases.

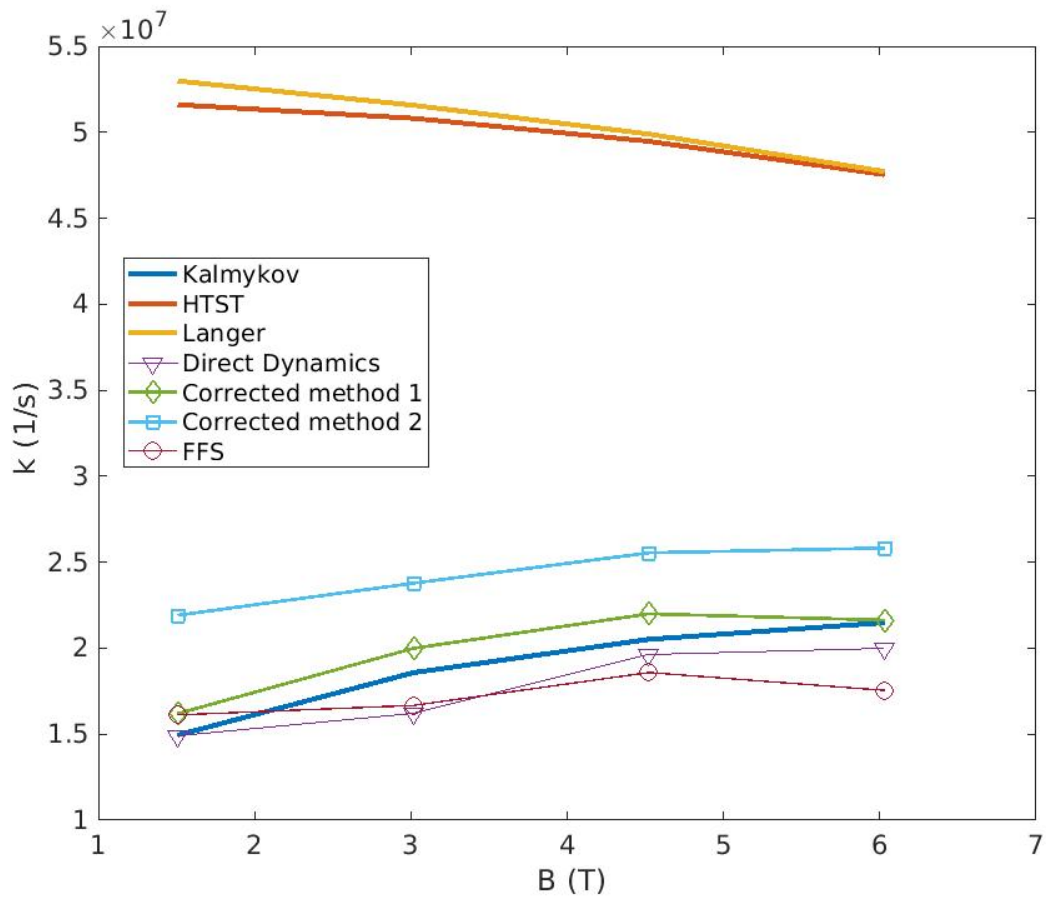


Figure 8: Results for the rate constant as a function of external field B when the damping parameter is fixed to $\alpha = 0.02$. The graph shows the results obtained with the different methods described above along with the results obtained by Forward Flux Sampling (FFS) in [6].

References

- [1] Pavel Bessarab. *Theoretical description of stability and transitions between magnetic states*. PhD thesis, University of Iceland, 2013.
- [2] Pavel F. Bessarab, Valery M. Uzdin, and Hannes Jónsson. Harmonic transition-state theory of thermal spin transitions. *Phys. Rev. B*, 85:184409, May 2012.
- [3] Peter Hänggi, Peter Talkner, and Michal Borkovec. Reaction-rate theory: fifty years after kramers. *Rev. Mod. Phys.*, 62:251–341, Apr 1990.
- [4] Yuri P. Kalmykov. The relaxation time of the magnetization of uniaxial single-domain ferromagnetic particles in the presence of a uniform magnetic field. *Journal of Applied Physics*, 96(2):1138–1145, 2004.
- [5] James Keck. Statistical investigation of dissociation cross-sections for diatoms. *Discuss. Faraday Soc.*, 33:173–182, 1962.
- [6] Christoph Vogler, Florian Bruckner, Bernhard Bergmair, Thomas Huber, Dieter Suess, and Christoph Dellago. Simulating rare switching events of magnetic nanostructures with forward flux sampling. *Phys. Rev. B*, 88:134409, Oct 2013.
- [7] Arthur F. Voter and Jimmie D. Doll. Dynamical corrections to transition state theory for multistate systems: Surface self-diffusion in the rare-event regime. *The Journal of Chemical Physics*, 82(1):80–92, 1985.